

The role of HD cooling in primordial star formation

Emanuele Ripamonti^{1*}

¹ *University of Groningen, Kapteyn Astronomical Institute, Postbus 800, 9700 AV Groningen, The Netherlands*

Submitted: June 2006; accepted: January 2007

ABSTRACT

The role of HD cooling in the formation of primordial objects is examined by means of a great number of 1-D models of the collapse of halos, exploring a wide range of masses and virialization redshifts. We find that HD has very little effect upon the critical mass separating the objects which are likely to form stars from those which are not. We also find that, once the proto-stellar collapse has started, HD effects are quite negligible.

Instead, HD effects can be important during the intermediate stage of gas fragmentation: objects below a certain mass scale ($\sim 3 \times 10^5 M_\odot$ at $z_{\text{vir}} = 20$ in our “fiducial” case) can be cooled by HD down to $T \sim 50 - 100$ K, whereas H_2 cooling never takes the gas below $T \sim 200$ K. The lower temperature implies a reduction of a factor ~ 10 in the Jeans mass of the fragmenting gas, and stars forming in such low-mass halos are probably less massive than their counterparts in larger halos. We estimate the importance of this mode of star formation through a variation of the Press-Schechter formalism, and find that it never exceeds the contribution of halos which are cooled by H_2 only. Halos where HD is important account at best for a fraction ~ 0.25 of the total primordial star formation. However, HD cooling might provide a channel through which long-lived low mass stars could be formed in primordial conditions.

Key words: stars: formation – molecular processes – cosmology: theory.

1 INTRODUCTION

Molecules play a decisive role in the formation of the first generations of luminous objects, because they provide the main cooling mechanism for primordial metal-free gas in small halos virializing at high redshift (*e.g.* Barkana & Loeb 2001; Bromm & Larson 2004; Glover 2004; Ciardi & Ferrara 2005; Ripamonti & Abel 2005).

The H_2 molecule has long been recognized (Saslaw & Zipoy 1967, Peebles & Dicke 1968, Matsuda, Sato & Takeda 1969) as the most important cooling agent in such conditions. Its cooling and chemical properties have been carefully studied (*e.g.* Hollenbach & McKee 1979; Palla, Salpeter & Stahler 1983 [PSS83]; Stancil, Lepp & Dalgarno 1996, 1998; Abel et al. 1997 [A97]; Galli & Palla 1998 [GP98], Glover, Savin & Jappsen 2006; Hirata & Padmanabhan 2006) and are a key component of all recent theoretical models and numerical investigations of the formation of the first objects (*e.g.* Tegmark et al. 1997 [T97]; Omukai & Nishi 1998; Bromm, Coppi & Larson 1999 [BCL99], 2002 [BCL02]; Abel, Bryan & Norman 2000, 2002 [ABN02]; Ripamonti et al. 2002 [R02], Yoshida et al. 2006 [Y06]).

Such studies suggest that primordial stars are more massive than their present-day counterparts, and that this

difference arises from the different cooling properties of metal-free and metal-enriched gas (Bromm et al. 2001; Omukai & Palla 2001, 2003; Schneider et al. 2002). A direct link seems to exist between the properties of H_2 cooling and the large fragment mass and the high proto-stellar accretion rate which are found to occur in simulations of primordial objects.

However, most of these studies consider H_2 as the only molecular coolant of primordial gas. This assumption might be quite critical, because of the close link between molecular and stellar properties. In fact, a number of chemical models of the primordial medium (Puy et al. 1993; GP98; Stancil, Lepp & Dalgarno 1998) have actually shown that, if the primordial gas cools below ~ 200 K, then HD molecules are likely to become the main cooling agents, despite their low number abundance. The cooling properties of HD and H_2 are quite different from each other, so this could have important consequences: for instance, in an HD-cooled gas, the Jeans mass (and the typical mass of primordial objects) would likely be reduced.

Such a possibly important role prompted further investigations of the HD cooling and chemistry (Flower 2000; Galli & Palla 2002 [GP02]; Lipovka, Nuñez-Lopez & Avila-Reese 2005) and especially of its effects on the properties of the first generations of stars (BCL99, BCL02; Uehara & Inutsuka 2000; Flower & Pineau des Forêts 2001; Nakamura

* E-mail: ripa@astro.rug.nl

& Umemura 2002; Johnson & Bromm 2006; Lipovka et al. 2005; Nagakura & Omukai 2005; Shchekinov & Vasiliev 2006; Y06).

All the studies which find that HD effects might be important were considering situations where the primordial gas was already “perturbed” by some kind of phenomenon, such as the shock due to the merger of two halos, or the radiation from the first stars. The “unperturbed” case was considered by the detailed simulations by BCL99, BCL02, and Y06, who included a treatment of HD chemistry and cooling in some of their simulations, and found that HD had minor effects at best. However, such results concern the evolution of single “typical” cases and do not rule out the existence of objects where HD cooling is actually important.

In this paper, we address the question of whether HD can be important during the birth of the *first generation* of luminous objects (that is, in *unperturbed* gas), with regard to the properties of the halos where they form, to the properties of fragmentation inside such halos, and to the characteristics of the proto-stellar collapse. This is done by means of spherically symmetric 1D calculations of the evolution of gas properties during the collapse of halos or proto-stars, through which we carry out an exploration of a large portion of the $z_{\text{vir}} - M_{\text{halo}}$ parameter space. Such exploration, combined with results from analytical models, allows us to give a quantitative estimate of the importance of HD-cooled objects.

This paper is organized as follows: in section 2 we describe the details of the 1D calculations; in section 3 we examine the results obtained from such calculations, and in section 4 we discuss their cosmological significance. Finally, in section 5 we summarize our conclusions.

Throughout all of this paper, we assume a flat Λ CDM cosmological model with parameters taken from the three years WMAP results reported by Spergel et al. 2006: $\Omega_{\Lambda} = 0.76$, $\Omega_{\text{m}} = 0.24$, $\Omega_{\text{b}} = 0.042$, $\Omega_{\text{DM}} \equiv \Omega_{\text{m}} - \Omega_{\text{b}} = 0.198$, $h = 0.73$. Furthermore, $\rho_0 \simeq 1.88 \times 10^{-29} h^2 \text{ g cm}^{-3}$ is the critical density of the universe,

2 METHOD

In order to assess the effects of HD in a wide range of cosmological environments, a method similar to that of T97 is adopted: rather than simulating a single “typical” object in great detail (as was done by BCL99, BCL02 and Y06), the “coarse” behaviour of a plethora of halos is probed, exploring the $z_{\text{vir}} - M_{\text{halo}}$ parameter space.

2.1 The 1D Code

The main tool employed in this paper is a 1D Lagrangian hydrodynamical spherically symmetric code, which follows the evolution of primordial gas inside and around DM halos, from the recombination epoch until well after the DM has virialized. Such code is described in R02 (see also Thoul & Weinberg 1995; and Omukai & Nishi 1998). Here we just outline the changes that were made in order to adapt it to our present purposes.

Table 1. List of considered reactions

#	Reaction	Reference
1	$\text{H}^+ + e^- \rightarrow \text{H} + \gamma$	A97/2 ^a GP98/H1 ^{a,b}
2	$\text{H} + \gamma \rightarrow \text{H}^+ + e^-$	GP98/H2 ^b
3	$\text{H} + e^- \rightarrow \text{H}^- + \gamma$	A97/7
4	$\text{H}^- + \gamma \rightarrow \text{H} + e^-$	GP98/H4
5	$\text{H} + \text{H}^- \rightarrow \text{H}_2 + e^-$	A97/8
6	$\text{H}^- + \text{H}^+ \rightarrow \text{H} + \text{H}$	A97/16
7	$\text{H} + \text{H}^+ \rightarrow \text{H}_2^+ + \gamma$	GP98/H8
8	$\text{H}_2^+ + \gamma \rightarrow \text{H} + \text{H}^+$	GP98/H9
9	$\text{H}_2^+ + \text{H} \rightarrow \text{H}_2 + \text{H}^+$	A97/10
10	$\text{H}_2 + \text{H}^+ \rightarrow \text{H}_2^+ + \text{H}$	GP98/H15
11	$\text{D}^+ + e^- \rightarrow \text{D} + \gamma$	A97/2 ^a GP98/D1 ^{a,b}
12	$\text{D} + \gamma \rightarrow \text{D}^+ + e^-$	GP98/D2 ^b
13	$\text{H}^+ + \text{D} \rightarrow \text{H} + \text{D}^+$	GP02/5
14	$\text{H} + \text{D}^+ \rightarrow \text{H}^+ + \text{D}$	GP02/6 ^c
15	$\text{D}^+ + \text{H}_2 \rightarrow \text{HD} + \text{H}^+$	GP02/2
16	$\text{HD} + \text{H}^+ \rightarrow \text{D}^+ + \text{H}_2$	GP02/4
17	$\text{H} + e^- \rightarrow \text{H}^+ + e^- + e^-$	A97/1
18	$\text{H} + \text{H} \rightarrow \text{H}^+ + \text{H} + e^-$	PSS83/9
19	$\text{He} + e^- \rightarrow \text{He}^+ + e^- + e^-$	A97/3
20	$\text{He}^+ + e^- \rightarrow \text{He} + \gamma$	A97/4
21	$\text{He}^+ + e^- \rightarrow \text{He}^{++} + e^- + e^-$	A97/5
22	$\text{He}^{++} + e^- \rightarrow \text{He}^+ + \gamma$	A97/6
23	$\text{D} + \text{H}_2 \rightarrow \text{HD} + \text{H}$	GP02/1 ^d
24	$\text{HD} + \text{H} \rightarrow \text{D} + \text{H}_2$	GP02/3 ^d
25	$\text{H} + \text{H} + \text{H} \rightarrow \text{H}_2 + \text{H}$	PSS83/4
26	$\text{H}_2 + \text{H} \rightarrow \text{H} + \text{H} + \text{H}$	PSS83/5
27	$\text{H} + \text{H} + \text{H}_2 \rightarrow \text{H}_2 + \text{H}_2$	PSS83/6
28	$\text{H}_2 + \text{H}_2 \rightarrow \text{H} + \text{H} + \text{H}_2$	PSS83/7

The reference codes give the paper from which the reaction coefficient was taken, and the number identifying each reaction in the corresponding paper.

^a We adopted the GP98 (case B) recombination rate before the turn-around redshift of each halo, when we switched to the A97 (case A) rate.

^b The coefficients given by GP98 for the ionization of H (and D) were transformed into reaction rates we could promptly use through eq. (1) of Sasaki & Takahara 1993.

^c As noted by Johnson & Bromm 2006, the reaction coefficient given by GP02 contains a typo; therefore, we actually use the original rate of Savin (2002).

^d When extrapolated to low temperature ($\lesssim 100$ K), these reaction rates become extremely large; since this is an artifact of the adopted fitting forms, and there is no experimental results at $T < 170$ K, we assume that at $T \leq 100$ K the rate coefficients of these reactions remain constant at the value we obtain for $T = 100$ K.

2.1.1 Chemistry

The chemical network of the original R02 code was revised and expanded. Now it follows the evolution of 12 species (the 9 “original” species, *i.e.* H, H^+ , H^- , H_2 , H_2^+ , He, He^+ , He^{++} , and e^- ; plus D, D^+ , and HD). The considered reactions are listed in Table 1. The network includes all the reactions for hydrogen and deuterium species which are in the *minimal model* of GP98, the collisional ionizations of hydrogen and helium, and two other deuterium reactions described by GP02 (these reactions were not part of the GP98 minimal model). Finally, there are the 3-body reactions of H_2 formation from PSS83. We stress that reactions 3 and 5

(13 and 15) are the main formation channel for H_2 (HD), unless the density is so high ($\rho \gtrsim 10^{-16} \text{ g cm}^{-3}$) that 3-body reactions (25 and 27) dominate.

As in the original code, the non-equilibrium chemistry of the considered species is solved at each time step through an implicit difference scheme.

It should be pointed out that, even if the rates given in Table 1 are fairly updated, their choice remains quite slippery: the uncertainties range from 10-20 per cent up to one order of magnitude in the worst cases (reactions 3, 4, 5, and 6, including the main formation channel of H_2). Glover et al. (2006) and Hirata & Padmanabhan (2006) find that the large uncertainties in these ill known reaction rates can have important effects on cosmological predictions; but also that the formation of the first protogalaxies from cold, neutral gas is relatively insensitive to the choice of the rates for these reactions. If so, the most problematic rate in our chemistry calculations is likely to be the one for reaction 15 (which is part of the main HD formation route): the value given by GP02 agrees within 20-30 per cent with that from Wang & Stancil (2002), but there exist measurements differing by almost a factor of 2 from these theoretical estimates (see fig. 3 of GP02, and fig. 14 of Wang & Stancil 2002). We will try to estimate the effects of this uncertainty by running a dedicated set of simulations (see Section 2.2.2).

It should also be noted that the rates of all the reactions which are caused by the interaction with a photon (2, 4, 8, and 12) only keep into account the effects of the CMB, while neglecting any extra radiation field which might be present (see Hirata & Padmanabhan 2006 for a possible effect of extra radiation).

2.1.2 Cooling

The original code included the treatment of cooling from H_2 roto-vibrational lines (including their radiative transfer) and from the CIE (Collision-Induced Emission) continuum. This was subject to several changes:

(i) The treatment of H_2 cooling was simplified in order to make the code faster: for this reason, we used the H_2 cooling rate from GP98, and treated the effects of line radiative transfer by using the methods devised in Ripamonti & Abel (2004) (in particular, of their equation 22); such methods are quite approximate, because the effects of line transfer are estimated only from the local density, whereas they depend also on temperature and velocity gradients. But they are adequate for the purposes of this paper.

(ii) The treatment of CIE cooling was switched off, as we never approach the density regime where it is important ($n \gtrsim 10^{14} \text{ cm}^{-3}$).

(iii) We included the cooling due to HD molecules, adopting the results of Lipovka et al. (2005), which consider also the effect of vibrational lines, and are valid in a wide range of temperatures ($40 \text{ K} \leq T \leq 2 \times 10^4 \text{ K}$) and densities ($1 \text{ cm}^{-3} \leq n_{\text{H}} \leq 10^8 \text{ cm}^{-3}$; this range can be easily extrapolated to both higher and lower densities)¹.

(iv) As we are concerned with a cosmological scenario, we included the cooling (or heating) from Compton scattering of CMB photons, and from Lyman α line cooling of atomic hydrogen. The adopted cooling rates per unit volume (from Rybicki & Lightman 1979 and Dalgarno & McCray 1972, respectively) are

$$\Lambda_{\text{C}}(T, T_{\gamma}) \simeq 1.0 \times 10^{-37} n_e T_{\gamma}^4 (T_{\gamma} - T) \text{ erg s}^{-1} \text{ cm}^{-3} \quad (1)$$

$$\Lambda_{\text{H}}(T) \simeq 7.5 \times 10^{-19} e^{-118348/T} n_e n_{\text{H}} \text{ erg s}^{-1} \text{ cm}^{-3} \quad (2)$$

where T , T_{γ} ($\simeq 2.725(1+z)$), n_e and n_{H} are the temperatures of the gas and of the cosmic background radiation (both in K), and the number densities of free electrons and H atoms (both in cm^{-3}), respectively.

(v) When the temperature of the gas is of the same order as that of the cosmic background radiation, the cooling rates from H_2 and HD can be substantially modified (see *e.g.* fig. 9 of GP02), as atoms and molecules become *heating* agents when $T < T_{\gamma}$. We account for the effects of the CMB upon the H_2 and HD cooling rates by estimating the *net* cooling rates through an adaptation of eq. (6) of Puy et al. (1993)²

$$\Lambda_{\text{net}, \text{H}_2}(T, T_{\gamma}) \simeq \Lambda_{\text{H}_2}(T) [1 - e^{T_{\text{H}_2}(\frac{1}{T} - \frac{1}{T_{\gamma}})}]. \quad (3)$$

$$\Lambda_{\text{net}, \text{HD}, j}(T, T_{\gamma}) \simeq \Lambda_{\text{HD}}(T) [1 - e^{T_{\text{HD}}(\frac{1}{T} - \frac{1}{T_{\gamma}})}]. \quad (4)$$

where $T_{\text{H}_2} \simeq 512 \text{ K}$ ($T_{\text{HD}} \simeq 128 \text{ K}$) is the excitation temperature of H_2 (HD). The CMB also affects the Lyman α cooling, but this is completely negligible, as $\Lambda_{\text{H}}(T)$ is extremely small for $T \sim T_{\gamma}$.

2.1.3 Dark Matter

The gravitational effects of Dark Matter (DM) were introduced in the code. The DM halo was assumed to be always spherically symmetric and concentric with the simulated region, whose central part represents the investigated halo. A DM mass of $M_{\text{DM}} = M_{\text{halo}} \Omega_{\text{DM}} / \Omega_{\text{m}}$ is assumed to be within a certain truncation radius R_{tr} , inside which the DM density profile is a truncated isothermal sphere with a flat core of radius R_{core} ; outside the truncation radius, the DM density is assumed equal to the cosmological average. So,

$$\rho_{\text{DM}}(r) = \begin{cases} \rho_{\text{core}} & \text{if } r \leq R_{\text{core}}; \\ \rho_{\text{core}}(r/R_{\text{core}})^{-2} & \text{if } R_{\text{core}} \leq r \leq R_{\text{tr}}; \\ \rho_0 \Omega_{\text{DM}} (1+z)^3 & \text{if } r \geq R_{\text{tr}}, \end{cases} \quad (5)$$

where the core density ρ_{core} is

$$\rho_{\text{core}} = M_{\text{DM}} \left[\frac{4\pi}{3} R_{\text{core}}^3 \left(\frac{3R_{\text{tr}}}{R_{\text{core}}} - 2 \right) \right]^{-1}, \quad (6)$$

as can be obtained by equating the DM mass within R_{tr} to M_{DM} .

The truncation and core radii were assumed to evolve in time, mimicking the results for the evolution of a simple *top-hat* fluctuation (see *e.g.* Padmanabhan 1993), and are described by the following equations

¹ We actually used the polynomial fit provided by Lipovka et al. (2005); the fit is quoted to be close to their original results for

² In the Puy et al. (1993) paper, the sign of the argument of the exponential is wrong because of a typographical error.

$$R_{\text{tr}}(z) = \begin{cases} \left(\frac{3}{4\pi} \frac{M_{\text{DM}}}{\rho_{\text{TH}}(z)} \right)^{1/3} & \text{if } z \geq z_{\text{ta}} \\ R_{\text{vir}} \left[2 - \frac{t(z)}{t(z_{\text{vir}}) - t(z_{\text{ta}})} \right] & \text{if } z_{\text{ta}} > z \geq z_{\text{vir}} \\ R_{\text{vir}} & \text{if } z < z_{\text{vir}} \end{cases} \quad (7)$$

$$R_{\text{core}}(z) = \begin{cases} R_{\text{tr}}(z) & \text{if } z \geq z_{\text{ta}} \\ R_{\text{vir}} \left[2 - \frac{(2-\xi)t(z)}{t(z_{\text{vir}}) - t(z_{\text{ta}})} \right] & \text{if } z_{\text{ta}} > z \geq z_{\text{vir}} \\ \xi R_{\text{vir}} & \text{if } z < z_{\text{vir}} \end{cases} \quad (8)$$

where $z_{\text{ta}} \simeq 1.5(1 + z_{\text{vir}}) - 1$ is the turn-around redshift, $t(z)$ is the time corresponding to redshift z , and the DM density inside the halo before z_{ta} is given by equations (23)³ and (24) of T97, which are a good approximation of the top hat results:

$$\rho_{\text{TH}}(z) = \rho_0 \Omega_{\text{DM}} (1+z)^3 \left[1 + \left(e^{\frac{1.9A}{1-0.75A^2}} - 1 \right) \right], \quad (9)$$

$$A = A(z) \equiv (1 + z_{\text{vir}})/(1 + z). \quad (10)$$

Finally, ξ (for which we will consider values in the range 0.01 – 0.2) is the ratio between the final size of the flat density core and the virial radius, which we define as

$$R_{\text{vir}} \equiv \frac{1}{2} R_{\text{tr}}(z_{\text{ta}}) = \frac{1}{2} \left(\frac{3}{4\pi} \frac{M_{\text{DM}}}{\rho_{\text{TH}}(z_{\text{ta}})} \right)^{1/3}. \quad (11)$$

Such a definition is unusual, but the difference with the most common definitions of the virial radius (*e.g.* Padamanabhan 1993) is less than 0.4 per cent.

The above equations divide the evolution of the DM profile in three stages: before the halo turn-around, it is reasonable to assume that the density profile within the halo is flat (therefore, $R_{\text{core}} = R_{\text{tr}}$). After the turn-around the density profile is evolved smoothly, reaching an equilibrium configuration at the virialization redshift; after that, the DM profile becomes completely static.

This is a crude model of the dark matter halo, but it is adequate for our purposes. We emphasize that the choice of a model with a *flat* core, rather than a cusp as in the NFW profile (Navarro, Frenk & White 1997), helps to ensure that the behaviour we observe near the centre is due to the self-gravity and hydrodynamics of the *simulated* gas, rather than to the *assumed* DM profile. However, in the following we will also discuss the effects of a cuspy NFW profile for the static post-virialization phase.

2.2 The models

2.2.1 Initial conditions

We start our computations at a very high redshift ($z = 1000$), when both the dark matter and baryonic overdensities are still very small, and it is perfectly reasonable to assume an uniform distribution of the gas (the effects of Compton drag further improve the accuracy of this assumption – see eq. 4.171 of Padmanabhan 1993). Furthermore, we simulate a region whose comoving initial radius is 10 times larger than that of the halo, in order to achieve a better modeling of the hydrodynamical effects, as this guarantees that the total mass in the simulated region is well above both

³ In the original reference (T97) this formula is affected by a typographical error, as the sign inside the exponential is wrong.

Table 2. Assumed chemical composition at $z=1000$

Species(X)	n_X/n_H ^a	Comments
H ⁰	0.9328	< 1 because H is partly ionized
H ⁺	0.0672	Sasaki & Takahara 1993 ^b
H ⁻	10 ⁻¹⁹	GP98, fig. 4
H ₂	10 ⁻¹³	GP98, fig. 4
H ₂ ⁺	10 ⁻¹⁸	GP98, fig. 4
He	0.0833	
He ⁺	10 ⁻²⁵	GP98, fig. 4
He ⁺⁺	0	
e ⁻	0.0672	from charge conservation
D ⁰	2.332×10^{-5}	(Romano et al. 2003) ^c
D ⁺	1.68×10^{-6}	(Romano et al. 2003) ^c
HD	2.5×10^{-18}	(Romano et al. 2003) ^c

^a n_H is the *total* abundance of H, including all species, *i.e.* $n_H = n_{H^0} + n_{H^+} + n_{H^-} + 2(n_{H_2} + n_{H_2^+}) + n_{HD}$.

^b from their model with $\Omega_0 = 1$, $\Omega_b = 0.05$, $h = 0.5$ (tab. 1); this value also agrees with the result of the RECFAST code (Seager, Sasselov & Scott 1999, 2000) for the flat Λ CDM cosmology we are assuming.

^c Romano et al. (2003) actually give the *total* abundance of D, $n_D = 2.5 \times 10^{-5} n_H$; we split this into the D⁰, D⁺ and HD abundances by assuming that $n_{D^+}/n_D = n_{H^+}/n_H$, and that $n_{HD}/n_D = n_{H_2}/n_H$.

the cosmological Jeans mass and the filtering mass (see *e.g.* Peebles 1993, and Gnedin 2000).

We assumed that at $z = 1000$ the gas temperature is the same as that of the CMB ($\simeq 2728$ K), that its density is equal to the cosmological average for baryons ($\rho_{\text{gas}}(z = 1000) \simeq 4.22 \times 10^{-22}$ g cm⁻²), and that the chemical abundances are those listed in Table 2.

2.2.2 Simulation sets

We ran several sets of simulations (listed in Table 3), covering halos with virialization redshifts in the range $10 \leq z_{\text{vir}} \leq 100$ and total (baryonic+dark matter) halo masses in the range $5 \times 10^3 M_\odot \leq M_{\text{halo}} \leq M_H(z_{\text{vir}})$. M_H is the minimum mass of the halos in which the cooling from atomic H is effective, that is, the minimum mass of halos with $T_{\text{vir}} \geq 10^4$ K

$$M_H(z_{\text{vir}}) \simeq 1.05 \times 10^9 M_\odot \left(\frac{\mu}{1.23} \right)^{-3/2} (1 + z_{\text{vir}})^{-3/2}, \quad (12)$$

where μ is the mean molecular weight of the primordial gas.

Each simulation set includes *two* runs for each $(z_{\text{vir}}, M_{\text{halo}})$ pair, differing only because HD cooling is either included or omitted. The results of the runs without HD cooling are used as a control sample. The models are based on the initial conditions described above, and consist of 150 shells, whose mass increases from the centre to the outskirts. The spacing was chosen in order to achieve sufficient mass “resolution” at the centre: the mass of the central shell is always $\sim 0.3 M_\odot$, which is a very small fraction ($\sim 10^{-3}$) of the mass of the fragments seen in the simulations of ABN02, BCL02, and Y06.

We ran several sets of simulations, in order to check the effects of the most uncertain parameters describing our initial conditions, such as the DM density profile:

Table 3. Summary of simulation sets

Set	DM profile	Abundances	Remarks
$\xi = 0.1$	Isothermal ^a ($\xi = 0.1$)	from Table 2	Fiducial
extra-D	Isothermal ^a ($\xi = 0.1$)	High ^c D, e ⁻ , H ⁺	Doubled rate of reaction 15
$\xi = 0.2$	Isothermal ^a ($\xi = 0.2$)	from Table 2	
$\xi = 0.05$	Isothermal ^a ($\xi = 0.05$)	from Table 2	
$\xi = 0.01$	Isothermal ^a ($\xi = 0.01$)	from Table 2	
NFW	NFW ^b ($c = 10$)	from Table 2	

^a Truncated isothermal, as described in section 2.1.3.

^b Before virialization, the DM profile is assumed to evolve as in the fiducial ($\xi = 0.1$) set.

^c For D, e⁻, and H⁺, twice the value given in Table 2. The other abundances given there are the same, except for H⁰ (which was reduced to 0.8656 in order to compensate the increase in H⁺).

(i) We check the influence of the concentration of the previously described truncated isothermal DM density profile by running four sets ($\xi = 0.2$, $\xi = 0.1$, $\xi = 0.05$, and $\xi = 0.01$) of simulations differing for the value of the ξ parameter. We will refer to the $\xi = 0.1$ set as to the “fiducial” set.

(ii) We check whether a cuspy density profile can lead to significantly different results by running a set of simulations (NFW) in which the post-virialization density profile within R_{vir} is described by a NFW profile with concentration parameter $c = 10$; in these models, the evolution of the DM density profile before virialization is the same as for the “fiducial” model.

(iii) We check whether HD effects depend strongly on the assumed abundances (at $z = 1000$) and on the uncertain rate of reaction 15 by running a set of simulations (extra-D) in which we double the initial values of both the electron (and H⁺) fraction given in Table 2 (to 0.1344), and the deuterium total abundance (to $n_{\text{D}}/n_{\text{H}} = 5 \times 10^{-5}$); we also assume that the rate of reaction 15 is twice as high as its standard value. All these changes favour HD formation, and this simulation set is mostly useful as an upper limit on the effects of HD (in the case that $\xi = 0.1$).

All the runs were stopped when a density $\rho_{\text{coll}} = 1.67 \times 10^{-19} \text{ g cm}^{-3} = 10^5 m_{\text{H}} \text{ cm}^{-3}$ is reached at some shell (generally at the centre), or when the simulation reaches $z_{\text{stop}} = 5$, whichever comes first. Our choice of ρ_{coll} ensures that the gas reaches densities where the first run-away collapse is taking place; furthermore, $\rho_{\text{coll}} \gg \rho_{\text{vir}}$, which ensures that the collapse is highly significant, and also that our results are quite independent of the exact value of ρ_{coll} . Instead, we chose $z_{\text{stop}} = 5$ because below that redshift the halos which are cooled by molecules are both cosmologically unimportant, and extremely unlikely to survive in the unperturbed (and neutral) conditions we are assuming.

3 RESULTS

3.1 Critical masses

Since the Compton heating due to residual free electrons largely dominates the thermal behaviour of the “average” IGM, the inclusion of HD cooling scarcely affects the chemical and thermal evolution of the IGM, even inside regions

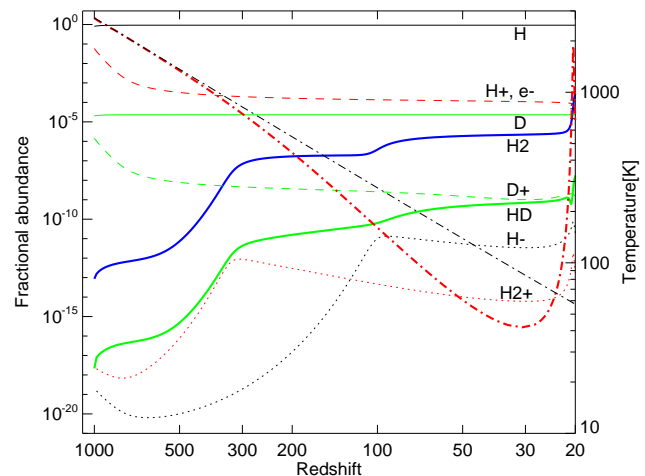


Figure 1. Chemical and thermal evolution between recombination and virialization of a $10^6 M_{\odot}$ halo with $z_{\text{vir}} = 20$, taken from the “fiducial” set of simulations. The left axis refers to the labelled lines, showing the abundance evolution of the various species: the abundances of H⁺ and e⁻ are always extremely close, and are represented by a single line; neutral and ionized He were omitted. The right axis refers to the two dot-dashed lines without labels, which show the evolution of the CMB and of the gas temperature (thin line and thick line, respectively). The results shown in this plot are almost independent of M_{halo} and of the inclusion of HD cooling, up to at least the turn around redshift $z_{\text{ta}} = 30.5$.

which will later virialize into halos, such as those shown in Fig. 1⁴.

Instead, HD cooling might affect the thermal evolution of the gas in a halo before and immediately after virialization, changing the *critical mass* which separates efficiently and inefficiently cooling halos (see *e.g.* T97).

Each of our simulated halos was classified as *collapsing* (or equivalently, efficiently cooling) or *non-collapsing* (inef-

⁴ Hirata & Padmanabhan 2006 have shown that the amount of H₂ which formed in the IGM through the H₂⁺ and the H⁻ channels (reactions 3, 5, 9, and 10 of Table 1) at $z \gtrsim 70$ might be substantially less than what is shown in Fig. 1. In the rest of this paper we neglect this uncertainty because in our simulations the bulk of H₂ forms inside the halos after they virialize, and the “background” abundance has very little effects on our results.

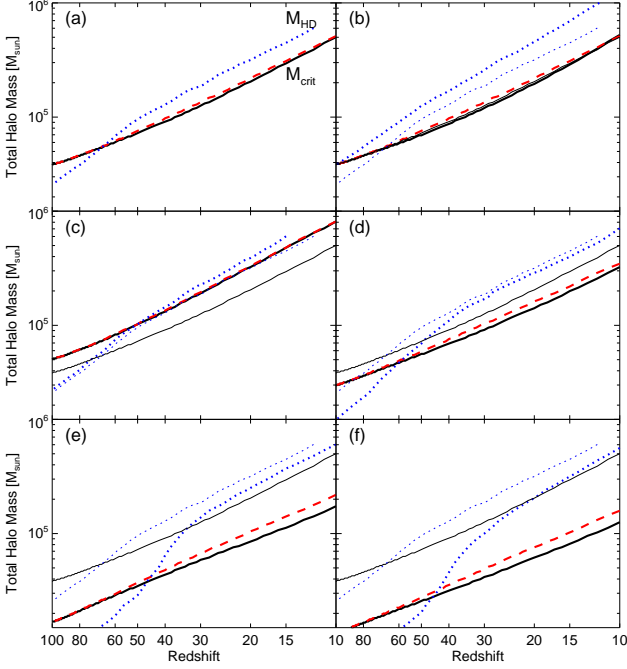


Figure 2. Evolution of the critical mass (M_{crit}), and of the mass below which HD becomes important (M_{HD}) as a function of the virialization redshift z_{vir} , for our six sets of simulations. Solid lines show the evolution of M_{crit} when HD cooling is included in the simulations, while dashed lines show the case where HD cooling is neglected; dotted lines show M_{HD} . Panels refer to the (fiducial) $\xi = 0.1$ set (a), to the extra-D set (b), to the $\xi = 0.2$ set (c), to the $\xi = 0.05$ set (d), to the $\xi = 0.01$ set (e), and to the NFW set (f). The results of the fiducial case are repeated as thin lines in all the panels, in order to facilitate the comparison between the various sets. M_{crit} is almost unaffected by the inclusion of HD cooling; however, the mass range between M_{HD} and M_{crit} becomes significant in the extra-D set, or if the DM halos are quite concentrated.

ficiently cooling), depending on whether it reaches a maximum density larger than ρ_{coll} in a less than an Hubble time, *i.e.* at a redshift $z_{\text{coll}} \gtrsim [0.63(1 + z_{\text{vir}})] - 1$.

Efficiently cooling halos have a high probability of forming luminous objects; this probability is much lower (but sometimes not completely negligible, as we show in the next section) for inefficiently cooling halos.

Our definition of collapsing halos is comparable to the “collapse criterion” of T97 (see their §5.1), so we use a similar notation and define $M_{\text{crit}}(z_{\text{vir}})$ as the minimum mass of an efficiently cooling halo virializing at z_{vir} .

In figure 2 we show the behaviour of $M_{\text{crit}}(z_{\text{vir}})$, comparing the results of the runs including HD cooling with those of the “control” runs. All the six sets of simulations are shown. In all cases HD has very little effect upon M_{crit} , as the solid and dashed curves of each simulation set are always close: models where the DM is quite concentrated exhibit slightly larger differences; but they never amount to more than 20 – 30%, even in the case of a NFW profile.

The reason of this result is that HD cooling can overcome H_2 cooling only when the temperature is quite low ($\lesssim 200$ K, see fig. 3). But the gas temperature at virialization is $T \simeq T_{\text{vir}} \sim 1000$ K, and HD can become important

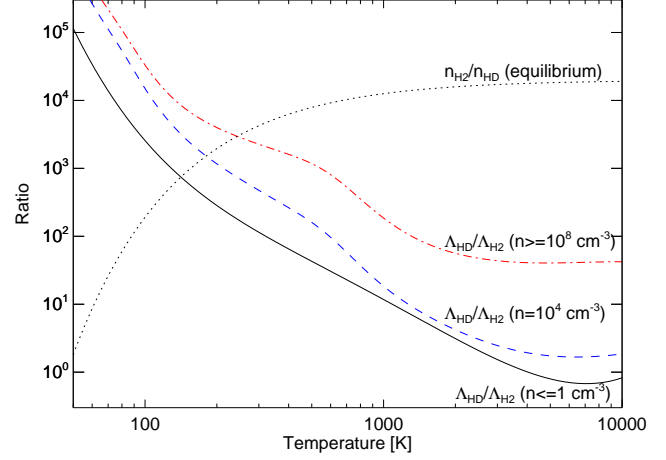


Figure 3. Ratio of the HD cooling per molecule to the H_2 cooling per molecule as a function of temperature at three different densities: 1 cm^{-3} (*i.e.* low density limit; solid line), 10^4 cm^{-3} (dashed line), and 10^8 cm^{-3} (*i.e.* high density limit; dot-dashed line). They are compared to the $n_{\text{H}_2}/n_{\text{HD}}$ ratio (dotted line) which can be expected if reactions 15 and 16 of Table 1 are at equilibrium (see *e.g.* of Shchekinov & Vasiliev 2006): if this assumption is correct, the intersections between this line and the other three lines mark the conditions where H_2 and HD are equally important coolants.

only *after* H_2 has lowered the gas temperature by a substantial factor, *i.e.* only if H_2 cooling is efficient in the first place. Such an explanation is confirmed by Figures 4 and 5: before virialization HD cooling might even exceed H_2 cooling, but remains negligible when compared to the effects of Compton scattering on free electrons; at virialization H_2 overcomes both the Compton (because the increase in density favours H_2 formation, reducing the number of free electrons at the same time) and the HD contribution (because the increase in temperature reduces the ratio $\Lambda_{\text{HD}}/\Lambda_{\text{H}_2}$, and also the ratio $n_{\text{HD}}/n_{\text{H}_2}$). So, HD cooling may become dominant only well after virialization, when H_2 has already reduced the temperature by a factor $\gtrsim 2$.

3.2 Fragmentation

The simulations clearly show that even if HD has very little effect on *which* halos cool, collapse, and form stars, it can affect *how* this happens. Actually, there are objects where HD cooling has no effect, and objects where the thermal evolution of the gas is deeply affected by HD.

In Figures 4 and 5 we show the evolution of the central properties in two halos chosen from the fiducial set. These halos have the same z_{vir} (20) but different mass ($M_{\text{halo}} = 2 \times 10^5, 10^6 M_{\odot}$). In each figure the results of runs with and without HD cooling are compared. In particular, we are interested in the evolution of the Jeans mass, which is taken to be (cfr. Peebles 1993)

$$M_J(T, \rho, \mu) = \frac{\pi}{6} \left(\frac{\pi k_B T}{G \mu m_p} \right)^{3/2} \rho^{-1/2} \simeq 50 M_{\odot} T^{3/2} \mu^{-3/2} n^{-1/2}. \quad (13)$$

In the case of the smaller halo (fig. 4) the final stages

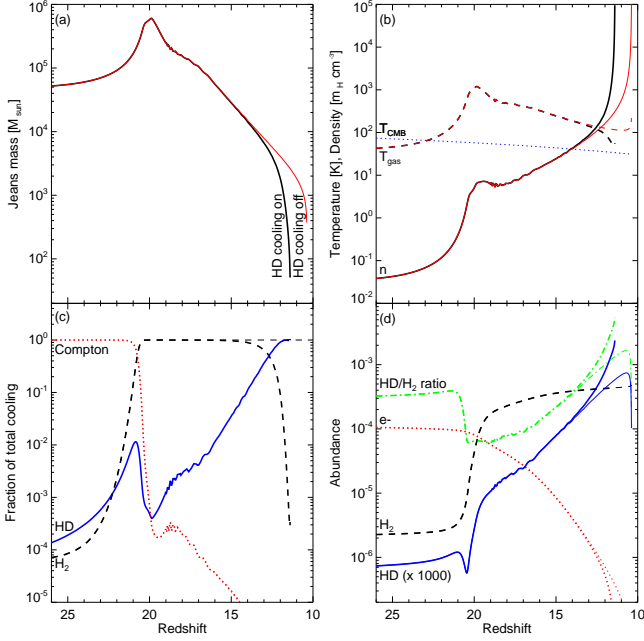


Figure 4. Evolution of the properties of the gas at the centre of an halo with $M_{\text{halo}} = 2 \times 10^5 M_{\odot}$ virializing at $z_{\text{vir}} = 20$ (taken from the fiducial set), as a function of redshift. In all panels, thick lines refer to models where HD cooling was included, whereas thin lines refer to models neglecting HD cooling. The properties shown are: Jeans mass (panel a); gas density and temperature (panel b; solid and dashed lines, respectively); fraction of the total cooling/heating due to HD, H_2 and Compton scattering (panel c; solid, dashed and dotted lines, respectively); fractional abundance of HD, H_2 and electrons (panel d; solid, dashed and dotted lines, respectively); the HD abundance shown here is 10^3 times larger the real value). In panel (b) the value of the CMB temperature is also shown (dotted line), and in panel (d) we additionally show the evolution of the $n_{\text{HD}}/n_{\text{H}_2}$ ratio (dot-dashed line).

of evolution differ, because HD cooling becomes dominant, anticipating the collapse (in this case ρ_{coll} is reached at $z \simeq 11.5$ rather than $z \simeq 10.3$), and, most importantly, lowering the gas temperature. In fact, the final temperature is ~ 70 K, *i.e.* 3-4 times lower than in the case where HD was neglected; as the Jeans mass is reduced by a factor ~ 10 , this behaviour strongly hints towards a change in the fragmentation properties of the gas inside an halo of this kind. On the other hand, in the case of the larger halo (fig. 5), the presence of HD makes no difference.

Figures 4 and 5 are illustrative of a general trend: HD is unimportant in the largest halos, but it becomes relevant at lower masses. In fact, when the largest halos are considered, the H_2 abundance just after virialization is above the threshold ($\sim 5 \times 10^{-4}$) identified by previous studies (*e.g.* T97) for H_2 cooling to be efficient. As H_2 sheds away most of the compressional heating, the collapse proceeds unimpeded; the gas remains at temperatures T above the 200 K “threshold” below which HD cooling becomes important (T usually reaches a minimum between 200 and 300 K, then slowly increases as the collapse proceeds). Instead, in smaller halos the H_2 abundance is below the threshold for efficiently dispersing the compressional heating, and the gas undergoes a stage of slow contraction and cooling; for example, in fig. 4 this phase lasts from $z \sim 20$ to $z \sim 13$. The “extra” time

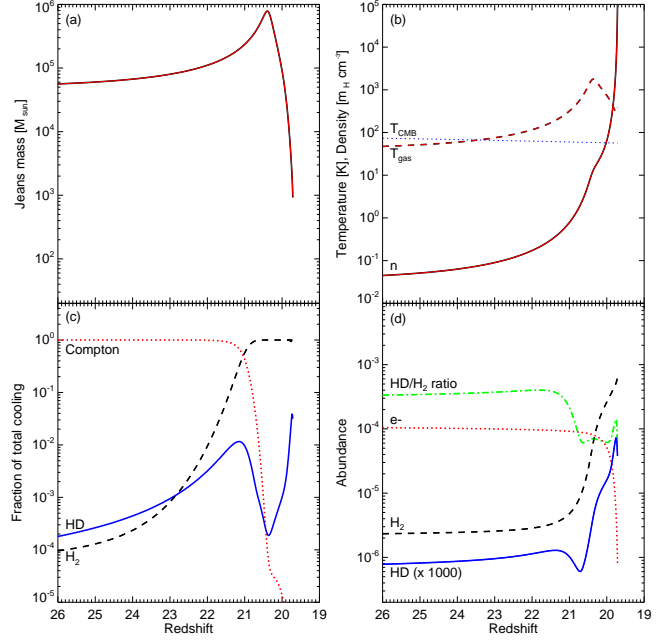


Figure 5. Evolution of the properties of the gas at the centre of an halo with $M_{\text{halo}} \simeq 10^6 M_{\odot}$ virializing at $z_{\text{vir}} = 20$, (taken from the fiducial set) as a function of redshift. See the caption of fig. 4 for a description of the panels and an explanation of the symbols. The absence of the thin lines associated with the case where HD cooling was not included is only apparent: in halos as massive as the one shown here, the gas evolution is not influenced by HD cooling, and the thin and thick tracks are perfectly superimposed.

spent in this phase allows a build up of HD (see especially panel (d) of fig. 4), until HD completely dominates the cooling and is finally able to “restart” the collapse.

In figure 2 we compare the critical mass $M_{\text{crit}}(z)$ to the mass $M_{\text{HD}}(z)$ below which HD cooling becomes important ($M_{\text{HD}}(z)$ was taken as the maximum mass where the inclusion of HD cooling takes the final gas temperature below 200 K, with a reduction of at least 25 per cent when compared to the value obtained when HD is neglected), for all the simulation sets we considered. The range between M_{HD} and M_{crit} (*i.e.* the collapsing halos where HD is likely to be important) is negligibly narrow for $\xi = 0.2$, but it gets wider when an higher D abundance is considered, or when the DM halos are assumed to be more concentrated than in the fiducial case (see also Section 4).

It is important to remark that our results are not in contradiction with the detailed simulations of BCL99, BCL02, and Y06, because all of them considered halos with masses in the range $0.5 - 1 \times 10^6 M_{\odot}$ at redshift ~ 20 , *i.e.* above M_{HD} . We must also remark that our results depend on the assumption that halos remain unperturbed, because mergers lead to dynamical heating, which could prevent the collapse also in halos with mass larger than M_{crit} (see Yoshida et al. 2003; Reed et al. 2005). Since the probability of mergers is particularly high in halos where HD is important (because of the long “build-up” phase), this effect is likely to reduce the fraction of halos where HD cooling is important (see also Section 4.2).

3.3 Proto-stellar collapse

Lipovka et al. (2005) suggested that HD cooling might be relevant also at relatively high densities and temperatures ($T \lesssim 3000$ K, $n \gtrsim 10^6$), a regime which is associated with proto-stellar collapse. Another reason to check this regime is that HD cooling might be in the optically thin regime even when the H_2 cooling is substantially reduced by radiative transfer effects.

In order to evaluate these effects, we re-ran some of our models with a better resolution (200 shells, mass of the central shell $\sim 10^{-3} M_\odot$) stopping them only after a density $n = 10^{13} \text{ cm}^{-3}$ was reached (after that, the fast increase of CIE cooling will overwhelm both H_2 and HD line cooling, see *e.g.* Ripamonti & Abel 2004). We explored 6 virialization redshifts ($z_{\text{vir}} = 10, 15, 20, 30, 50, 100$), always choosing an halo mass of $10^6 M_\odot$, above both $M_{\text{crit}}(z)$ and $M_{\text{HD}}(z)$: here we ignore halos where HD can affect fragmentation, because otherwise we cannot have a meaningful comparison with a model where HD cooling was neglected.

Again, by comparing simulations with and without HD cooling, (see *e.g.* fig. 6) we find that HD causes no difference also in this phase of the formation of a primordial star. The main reason is that the ratio $n_{\text{HD}}/n_{\text{H}_2}$ decreases with temperature (at equilibrium, $n_{\text{HD}}/n_{\text{H}_2} \propto e^{-\frac{465 \text{ K}}{T}}$, see Shchekinov & Vasiliev 2006), and so does the ratio of HD cooling per molecule to H_2 cooling per molecule. Furthermore, radiative transfer effects become important only when the H_2 fraction is already of the order of 1, implying $n_{\text{HD}}/n_{\text{H}_2} \lesssim 2n_{\text{D}}/n_{\text{H}} \simeq 5 \times 10^{-5}$ (10^{-4} if the abundances of the “extra-D” set are considered): this difference is simply too large to be compensated by the radiative transfer effects on H_2 cooling efficiency, especially at the relatively high temperatures (~ 1000 K) typically associated with the high-density phases of the collapse.

We emphasize that the above calculations always assumed the optically thin limit for HD cooling. We have not checked whether this is correct, but our results will not change even if it is not: in fact, the treatment of radiative transfer would then yield an effective HD cooling rate which is *lower* than what we assumed.

4 DISCUSSION

In the previous section we showed that in the standard Λ CDM model the main effect that HD might exert upon the evolution of unperturbed primordial halos is to reduce the typical stellar mass in objects below a certain mass $M_{\text{HD}}(z_{\text{vir}})$. Here, we investigate whether this “HD-dominated” regime of star formation is cosmologically relevant or not. This is done by comparing the mass of the stars which formed in halos affected by HD cooling, and in halos where only H_2 (or H) cooling was important.

4.1 Rates of formation and survival of objects

We base our estimates on a variation of the Press-Schechter formalism (Press, Schechter 1974), namely the extended Press-Schechter (EPS) formulae of Sheth & Tormen (1999) [ST99], which was found to be in reasonable agreement with the results of numerical simulations of the formation of very

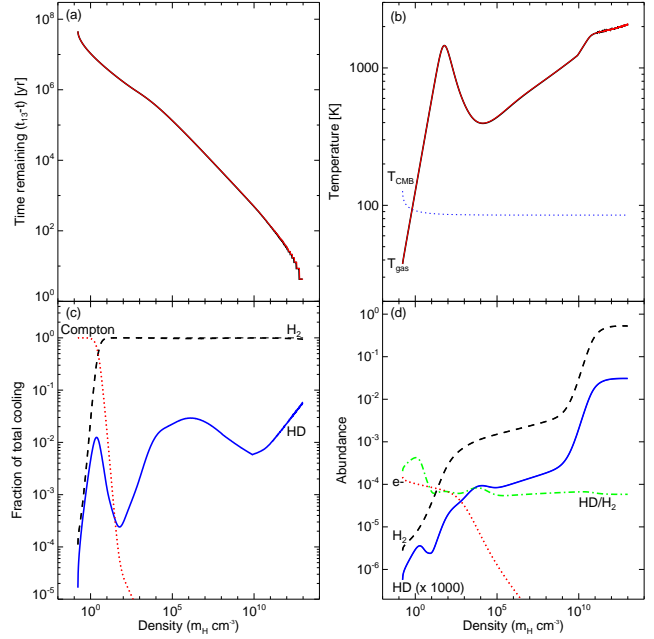


Figure 6. Evolution of the properties of the gas at the centre of an halo with $M_{\text{halo}} \simeq 10^6 M_\odot$ virializing at $z_{\text{vir}} = 30$ (taken from the fiducial set), as a function of central density. Panels (c) and (d) are the same as in figs. 4 and 5, except that the X-axis shows the gas central density, rather than the redshift. Panel (a) shows the time at which each density is reached, expressed as the time ($t_{13} - t$) remaining before reaching a density $10^{13} m_H \text{ cm}^{-3}$ at time t_{13} . Panel (b) shows the temperature evolution of the gas (solid lines) and of the CMB (dotted line). As in fig. 5, the absence of the thin lines (corresponding to the case where HD cooling was not considered) is only apparent: the results with and without HD are almost identical. Finally, the increase in the fraction of total cooling due to HD at high densities (panel c) is due to radiative transfer effects reducing the H_2 cooling efficiency; such effects are not considered for HD, so the high density part of the solid curve in panel (c) should be considered an upper limit.

early objects by Gao et al. (2005; see also Jenkins et al. 2001, Reed et al. 2003, Gao et al. 2004, Springel et al. 2005).

Such formulae can be treated in the same way as Sasaki (1994) did for the original Press-Schechter, leading to similar results: the comoving number density of virialized halos in the mass range between m and $m + dm$ at redshift z is

$$N_{\text{ST}}(m, z) = \left[\frac{\rho_0}{m} \left(\frac{2a}{\pi} \right)^{1/2} \left(-\frac{1}{\sigma(m)^2} \frac{d\sigma}{dm} \right) A \delta_c \right] \times \frac{1 + (a\nu)^{-p}}{D(z)} e^{-\frac{a\nu}{2}} \quad (14)$$

where $a = 0.707$, $A = 0.322$ and $p = 0.3$ are the parameters given by ST99 (instead, $a = 1$, $A = 0.5$, $p = 0$ correspond to a “standard” Press Schechter function), $\sigma(m)$ is the value of the root mean squared fluctuation in spheres that on average contain a mass m , $\delta_c \simeq 1.686$ is the overdensity threshold for the collapse, $D(z)$ is the growth function of perturbations (see Peebles 1993), and

$$\nu(m, z) \equiv \frac{\delta_c^2}{D(z)^2 \sigma(m)^2}. \quad (15)$$

The time derivative of eq. (14) is

$$\dot{N}_{\text{ST}}(m, z) = -\frac{dD}{dz} \frac{dz}{dt} \frac{1}{D} \left(1 - a\nu - 2p \frac{(a\nu)^{-p}}{1 + (a\nu)^{-p}} \right) \times N_{\text{ST}}(m, z) \quad (16)$$

and by following Sasaki 1994 (in particular in the assumption that the destruction rate of halos has no characteristic mass scale) we get that the formation rate is given by

$$\dot{N}_{\text{form}}(m, z) = \frac{dD}{dz} \frac{dz}{dt} \frac{1}{D} \frac{a\nu + (a\nu)^{1-p} - 2p}{1 + (a\nu)^{-p}} N_{\text{ST}}(m, z) \quad (17)$$

and also that the probability that an object which exists at z' survives until redshift z ($z < z'$) without merging is

$$p(z', z) = \left[\frac{D(z')}{D(z)} \right]^{1-2p} \simeq \left[\frac{1+z}{1+z'} \right]^{1-2p} \quad (18)$$

where the last equality is strictly valid only in an Einstein-de Sitter universe with $\Omega_m = 1$.

4.2 Mass fractions

The results of our simulations can be interpolated in order to get an estimate of the function $z_{\text{coll}}(m, z_{\text{vir}})$, *i.e.* of the redshift at which the collapse of the gas inside an halo of mass m that virialized at z_{vir} has proceeded far enough for star formation to occur; from the same data, we can also estimate a correlated quantity, *i.e.* the minimum mass $M_{\text{min}}(z_{\text{vir}}, z)$ that an unperturbed halo which virialized at z_{vir} must have in order to have formed stars before redshift z . These functions can be combined with the above equations (17) and (18) in order to find the mass fractions in object-forming halos of various kinds (HD-cooled, H_2 -cooled, H-cooled) as a function of redshift. For example, the fraction of mass that at redshift z is in halos which have produced (or are producing) stars through HD-dominated cooling is

$$f_{\text{HD}}(z) = \int_{z_1}^z dz_{\text{vir}} \frac{dt}{dz_{\text{vir}}} \int_{M_{\text{HD},1}}^{M_{\text{HD},2}} dm \frac{m}{\rho_0} \dot{N}_{\text{form}}(m, z_{\text{vir}}) p(z_{\text{vir}}, z), \quad (19)$$

where $z_1 = 100$ is the maximum considered redshift (we assume that the contribution to the star-forming density of halos from redshift higher than z_1 is negligible), and

$$M_{\text{HD},1} = \min(M_{\text{HD}}(z_{\text{vir}}), M_{\text{min}}(z_{\text{vir}}, z)), \quad (20)$$

$$M_{\text{HD},2} = M_{\text{HD}}(z_{\text{vir}}) \quad (21)$$

We note that the $p(z_{\text{vir}}, z)$ factor in eq. (19) excludes all the halos which experienced a major merger between z_{vir} and z ; this is a very approximate way of accounting for the effects of dynamical heating (Yoshida et al. 2003; Reed et al. 2005). Some of these excluded halos (namely, the ones undergoing a merger at a redshift between their z_{coll} and z) actually formed stars in the HD regime. This effect could be included in the calculation by changing the probability factor into $p(z_{\text{vir}}, \max(z, z_{\text{coll}}(m, z_{\text{vir}})))$. However, the difference between the two probabilities is relatively small: in the most extreme case (*i.e.* $z_{\text{vir}} = z_{\text{coll}} = 100$; $z = 10$) $p(z_{\text{vir}}, z_{\text{coll}})/p(z_{\text{vir}}, z) \simeq 2.41$, whereas for much more typical values of z_{vir} , z_{coll} , and z the correction factor is $\lesssim 1.5$, which is too small to alter the qualitative conclusions that can be reached through eq. (19).

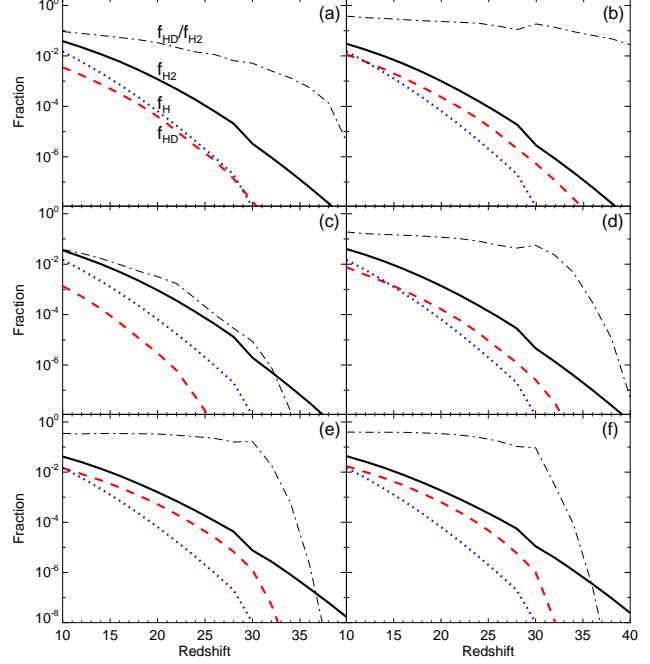


Figure 7. Evolution of the fraction of mass inside halos which were able to form stars within a given redshift. Solid lines: mass inside H_2 -cooled halos; dashed lines: mass inside HD-cooled halos; dotted lines: mass inside H-cooled halos; dot-dashed lines: ratio between the masses inside HD-cooled halos and H_2 -cooled halos. Panels refer to different sets of simulations, and are in the same order as in Fig. 2.

The mass fractions $f_{\text{H}_2}(z)$ and $f_{\text{H}}(z)$ (due respectively to objects where H_2 cooling and atomic H cooling is dominant) can be found by simply changing the limits of the mass integration inside eq. (19) to

$$M_{\text{H}_2,1} = \min(M_{\text{H}}(z_{\text{vir}}), \max(M_{\text{HD}}(z_{\text{vir}}), M_{\text{min}}(z_{\text{vir}}, z))), \quad (22)$$

$$M_{\text{H}_2,2} = M_{\text{H}}(z_{\text{vir}}) \quad (23)$$

and to

$$M_{\text{H},1} = \max(M_{\text{H}}(z_{\text{vir}}), M_{\text{min}}(z_{\text{vir}}, z)), \quad (24)$$

$$M_{\text{H},2} = \infty. \quad (25)$$

We calculated f_{HD} , f_{H_2} and f_{H} by taking the $\sigma(m)$ and $D(t)$ functions given in Eisenstein & Hu 1998. In fig. 7 we compare their redshift evolution. It is apparent that $f_{\text{HD}} < f_{\text{H}_2}$ at all redshifts and in all the cases we are considering. However, there is a substantial difference between the various simulation sets. In the least concentrated case ($\xi = 0.2$) the amount of star formation through the HD cooling regime is likely negligible, never exceeding 4 per cent of the total and rapidly decreasing when going to high redshifts. Instead, when the DM profiles are assumed to be moderately or highly concentrated ($\xi \lesssim 0.05$, or NFW profile), the difference between the HD and the H_2 channels for star formation reduces to a factor ~ 3 ; it is also essentially constant between $z = 10$ and $z = 30$, even if the efficiency of the HD channel rapidly drops at $z \gtrsim 30$ (a behaviour which could be expected from fig. 2); the fiducial set is somewhat in the middle, while the results from the extra-D set resem-

ble the ones we obtained for moderately concentrated DM profiles, except that the drop in $f_{\text{HD}}/f_{\text{H}_2}$ is much slower.

5 SUMMARY AND CONCLUSIONS

In this paper we examined the possible effects of HD cooling upon the most popular scenarios for the formation of first objects.

We found that HD cooling has very little effect upon the evolution of a halo before and during virialization, so that the critical mass M_{crit} separating star-forming and non-star-forming halos is scarcely affected. Similarly, we found that HD is even less important when the first phases of proto-stellar collapses are considered. Both these conclusions are quite independent of the shape of DM profiles, and of the exact abundance of Deuterium.

The most interesting of our results is that HD can influence the fragmentation process of primordial gas clouds into stars. In fact, our simulations show that in halos with masses just above M_{crit} , HD cooling dominates the phases of gas collapse when fragmentation is likely to take place, significantly reducing the gas temperature, the Jeans mass, and probably also the typical mass of fragments. If so, HD cooling could open a channel for the formation of relatively low mass stars even in metal-free gas.

We then employed a simple analytical model, based on the extended Press-Schechter formalism, in order to estimate the importance of this “HD mode” of star formation. A comparison with the common “H₂-only” mode of primordial star formation shows that the HD mode is always sub-dominant. However, its importance depends on the detailed DM density profile, on D abundance, and on the rate of HD formation. If DM profiles are assumed to be relatively loose, and if we take the “standard” values for D abundance and HD formation rate (as in our simulation sets $\xi = 0.2$ and $\xi = 0.1$), the range of halo masses where HD is important is quite narrow, and the number of stars whose formation is triggered by HD cooling is probably negligible. Instead, in the case of quite concentrated profiles, and/or of higher D abundances and HD formation rate (such as in our $\xi = 0.05$, $\xi = 0.01$, NFW, and extra-D simulations sets), HD dominated halos should account for about one quarter of all primordial star formation, at least if we are not underestimating too much the effects of dynamical heating.

We remark that there exist at least two mechanisms which could boost the importance of HD for primordial star formation. First of all, it is not unreasonable to expect that the star formation efficiency is higher for the halos which form stars through HD than for those where HD is unimportant. This is because the lower typical stellar mass should imply a weaker feedback.

A second possibility comes from considering that the ratio of HD to H₂ (and with it the mass range where HD cooling is important) is quite enhanced when the abundance of free electrons is higher than in the standard case (see *e.g.* Nagakura & Omukai 2005, O’Shea et al. 2005, Johnson & Bromm 2006, Yoshida 2006, even if all of them consider a different scenario). This might happen because of DM annihilations or decays (Ripamonti, Mapelli & Ferrara 2006), or, less exotically, because of the influence of nearby ioniz-

ing sources (*e.g.* accreting black holes, as in Zaroubi & Silk 2005).

6 ACKNOWLEDGEMENTS

The author thanks M. Mapelli, T. Abel, S. Zaroubi, E. Vasiliev, and M. Colpi for useful discussions in the preparation of this paper, and acknowledges support from the Netherlands Organization for Scientific Research (NWO) under project number 436016.

REFERENCES

- Abel T., Anninos P., Zhang Y., Norman M.L., 1997, *NewA*, 2, 181 [A97]
- Abel T., Bryan G.L., Norman M.L., 2000, *ApJ* 540, 39 [ABN00]
- Abel T., Bryan G.L., Norman M.L., 2002, *Science*, 295, 93 [ABN02]
- Barkana R., Loeb A., 2001, *Physics Reports*, 349, 125
- Bromm V., Larson R.B., 2004, *ARAA*, 42, 79
- Bromm V., Coppi P.S., Larson R.B., 1999, *ApJ*, 527L, 5 [BCL99]
- Bromm V., Coppi P.S., Larson R.B., 2002, *ApJ*, 564, 23 [BCL02]
- Bromm V., Ferrara A., Coppi P.S., Larson R.B., 2001, *MNRAS*, 328, 969
- Ciardi B., Ferrara A., 2005, *Space Science Reviews*, 116, 625
- Dalgarno A., McCray R.A., 1972, *ARAA*, 10, 375
- Eisenstein D.J., Hu W., 1998, *ApJ*, 496, 605
- Flower D.R., 2000, *MNRAS*, 318, 875
- Flower D.R., Pineau des Forêts G. 2001, *MNRAS*, 323, 672
- Galli D., Palla F., 1998, *A&A*, 335, 403 [GP98]
- Galli D., Palla F., 2002, *Planetary and Space Science*, 50, 1197 [GP02]
- Gao L., Loeb A., Peebles P.J.E., White S.D.M., Jenkins A., 2004, *ApJ*, 614, 17
- Gao L., White S.D.M., Jenkins A., Frenk C.S., Springel V., 2005, *MNRAS*, 363, 379
- Glover S.C.O., 2004, *Space Science Reviews*, 117, 445
- Glover S.C., Savin D.W., Jappsen A.-K., 2006, *ApJ*, 640, 553
- Gnedin N.Y., 2000, *ApJ*, 542, 535
- Hirata C.M., Padmanabhan N., 2006, preprint (astro-ph/0606437)
- Hollenbach D., McKee C.F., 1979, *ApJS*, 41, 555
- Jenkins A., Frenk C.S., Pearce F.R., Thomas P.A., Colberg J.M., White S.D.M., Couchman H.M.P., Yoshida N., 2001, *MNRAS*, 321, 372
- Johnson J.L., Bromm V., 2006, *MNRAS*, 366, 247
- Lipovka A., Nuñez-Lopez R., Avila-Reese V., 2005, 361, 850
- Matsuda T., Sato H., Takeda H., 1969, *Progr. Theor. Phys.*, 42, 219
- Nagakura T., Omukai K., 2005, *MNRAS*, 364, 1378
- Nakamura F., Umemura M., 2002, *ApJ*, 569, 549
- Navarro J.F., Frenk C.S., White S.D.M., 1997, *ApJ*, 490, 493
- Omukai K., Nishi R., 1998, *ApJ*, 508, 141
- Omukai K., Palla F., 2001, *ApJ*, 561L, 55
- Omukai K., Palla F., 2003, *ApJ*, 589, 677
- O’Shea B.W., Abel T., Whalen D., Norman M.L., 2005, *ApJ*, 628L, 5
- Padmanabhan T., 1993, “Structure formation in the universe”, Cambridge University Press, Cambridge(UK)
- Palla F., Salpeter E.E., Stahler S.W., 1983, *ApJ*, 271, 632 [PSS83]
- Peebles P.J.E., “Principles of Physical Cosmology”, Princeton University Press, Princeton, NJ (USA)
- Peebles P.J.E., Dicke R.H., 1968, *ApJ*, 154, 891
- Press W.H., Schechter P., 1974, *ApJ*, 187, 425

- Puy D., Alecian G., Le Bourlot J., L  orat J., Pineau des For  ts G., 1993, *A&A*, 267, 337
- Reed D.S., Gardner J., Quinn T., Stadel J., Fardal M., Lake G., Governato F., 2003, *MNRAS*, 346, 565
- Reed D.S., Bower R., Frenk C.S., Gao L., Jenkins A., Theuns T., White S.D.M., 2005, *MNRAS* 363, 393
- Ripamonti E., Haardt F., Ferrara A., Colpi M., 2002, *MNRAS* 334, 401 [R02]
- Ripamonti E., Abel T., 2004, *MNRAS*, 348, 1019
- Ripamonti E., Abel T., 2005, preprint (astro-ph/0507130)
- Ripamonti E., Mapelli M., Ferrara A., 2006, preprint (astro-ph/0606483)
- Romano D., Tosi M. Matteucci F., Chiappini C., 2003, *MNRAS*, 346, 259
- Rybicki G.B., Lightman A.P., 1979, “Radiative Processes in Astrophysics”, Wiley, New York
- Sasaki S., 1994, *PASJ*, 46, 427 [S94]
- Sasaki S., Takahara F., 1993, *PASJ*, 45, 655
- Saslaw W.C., Zipoy D., 1967, *Nature*, 216, 976
- Savin W.D., 2002, *ApJ*, 566, 599
- Schneider R., Ferrara A., Natarajan P., Omukai K., 2002, *ApJ*, 571, 30
- Seager S., Sasselov D.D., Scott D., 1999, *ApJ*, 523L, 1
- Seager S., Sasselov D.D., Scott D., 2000, *ApJS*, 128, 407
- Shchekinov Y.A., Vasiliev E.O., 2006, *MNRAS*, 368, 454
- Sheth R.K., Tormen G., 1999, *MNRAS*, 308, 119 [ST99]
- Spergel D.N. et al. , 2006, preprint (astro-ph/0603449)
- Springel V. et al. , 2005, *Nature*, 435, 629
- Stancil P.C., Lepp S., Dalgarno A., 1996, *ApJ*, 458, 401
- Stancil P.C., Lepp S., Dalgarno A., 1998, *ApJ*, 509, 1
- Tegmark M., Silk J., Rees M., Blanchard A., Abel T., Palla F., 1997, *ApJ*, 474, 1 [T97]
- Thoul A.A., Weinberg D.H., 1995, *ApJ*, 442, 480
- Uehara H., Inutsuka S., 2000, *ApJ*, 531L, 91
- Wang J.G., Stancil P.C., 2002, *Physica Scripta*, 96, 72
- Yoshida N., 2006, *NewA* 50, 19
- Yoshida N., Abel T., Hernquist L., Sugiyama N., 2003, *ApJ* 592, 645
- Yoshida N., Omukai K., Hernquist L., Abel T., 2006, preprint (astro-ph/0606106)
- Zaroubi S., Silk J., 2005, *MNRAS*, 360L, 64